SIMULATION ANALYSIS AND EXPERIMENT OF CLEANING MECHANISM FOR TRACK-TYPE COMBINE HARVESTER BASED ON CFD-DEM
/
基于 *CFD-DEM* 的履带式联合收获机清选装置仿真分析与试验

Hongda ZHAO[1), Xianghao LI[1),' Yongli ZHAO[1),' Shaochuan LI[1), Peisong DIAO[1*)]
[1)College of Agricultural Engineering and Food Science, Shandong University of Technology, Zibo, Shandong, 255000, China
E-mail: dps2003@163.com
Corresponding author: Peisong Diao

ABSTRACT
This research aims to solve the problem of material accumulation on the screen surface of the cleaning device of tracked combine harvester and proposes an innovative solution of designing a pre-screening device based on the traditional cleaning device. The problem of material accumulation on the screen surface is improved, which in turn enhances the cleaning efficiency. In this study, CFD-DEM coupled simulation technology is used to simulate and analyse the cleaning device, and the effects of airflow velocity, vibration frequency and amplitude on the cleaning effect are explored, and the impurity content and loss rate are used as evaluation indexes. Through orthogonal experimental analysis, the optimal parameter combination of the cleaning device was determined as airflow velocity 11 m/s, vibration frequency 9 Hz, amplitude 30 mm, impurity content rate 2.10% and loss rate 1.62%. The experimental results show that increasing the pre-screening device can significantly improve the material separation effect, reduce the loss and improve the cleaning efficiency.

摘要
本研究旨在解决履带式联合收获机清选装置的筛面物料堆积问题，提出了在传统清选装置基础上设计预筛装置的创新方案。改善了物料在筛面上的堆积问题，进而提升清选效率。本研究采用 CFD-DEM 耦合仿真技术，对清选装置进行模拟分析，探讨了风速、振频、振幅对清选效果的影响，并以含杂率和损失率作为评价指标。通过正交实验分析，确定了清选装置的最优参数组合为风速 11 m/s，振频 9Hz，振幅 30mm。含杂率为 2.10%，损失率为 1.62%。实验结果表明，增加预筛装置能够显著改善物料分离效果，减少损失，提高清选效率。

INTRODUCTION

Combine harvesters are a vital component of contemporary agricultural practices, facilitating the integration of numerous processes, including cutting, conveying, threshing, separating, cleaning, and grain collection, into a single operation. Among the various essential components of the combine harvester, the cleaning system is undoubtedly one of the most crucial. The performance of the combine harvester is significantly influenced by key structural parameters, which in turn impact the operational quality and harvesting efficiency of the machine.

The stability of the combine harvester's operation allows the vibration sieve in the cleaning unit to be designed with a wider range of amplitude and frequency adjustments, rendering it suitable for high humidity and high-viscosity soil conditions. This ensures that high cleaning efficiency is maintained even in complex environments. However, these challenging conditions also give rise to issues such as material accumulation on the sieve surface and an increased risk of sieve clogging, which ultimately affects cleaning efficiency.

To address the issues of material accumulation and decreased cleaning efficiency, *Zhang H. et al., (2022),* combination of numerical simulation and experimental validation was employed to optimise the design of the cleaning device, resulting in a notable enhancement in the separation of grains. *Li Hongchang et al., (2012),* conducted computational fluid dynamics (CFD) and discrete element method (DEM) numerical simulations on the movement of materials over the vibrating screen of an air-screen cleaning unit. Furthermore, *Guo Shuangjiang et al., (2021),* coupled EDEM and Fluent to find the optimum operating parameters of the flushing unit. In response to these challenges, this study proposes an improved solution in the form of the addition of a pre-screening device to the traditional cleaning unit.

Hongda ZHAO, M.S. Stud, Xianghao LI, M.S. Stud.; Yongli ZHAO, M.S. Stud.; Shaochuan LI, Ph.D Stud.; Peisong DIAO professor Dr.

By optimising the structural design of the pre-screening device and the operational parameters of the cleaning unit, the airflow distribution on the sieve surface is improved, which in turn reduces material accumulation and decreases the workload of the vibrating screen, thereby further enhancing cleaning efficiency. It is anticipated that the introduction of the pre-screening device will facilitate preliminary separation of materials prior to their entry into the vibrating screen. This is expected to result in a reduction in the load on the vibrating screen, thereby enhancing the efficiency of the cleaning process.

In order to conduct a comprehensive analysis and validation of the performance of the enhanced cleaning system, this paper employs a simulation approach that integrates Computational Fluid Dynamics (CFD) and the Discrete Element Method (DEM). In recent years, a considerable number of researchers have conducted a variety of studies, resulting in notable advancements. For example, *Christian Korn et al., (2017),* present a verification of the feasibility of the simulation model and an identification of potential avenues for improvement through a combination of numerical simulation and experimental comparison. *Xu Lizhang et al., (2014),* from Jiangsu University, employed a two-phase solid-liquid flow method to simulate and analyse the cleaning system of a rice harvester. *Liang Zhenwei et al., (2018),* and colleagues from Jiangsu University employed a two-phase gas-solid flow model in conjunction with practical test bench methods to enhance several pivotal factors of the fan in a multi-duct cleaning system. This resulted in a reduction of the impurity and loss rates by 0.5%. These studies primarily concentrate on the optimisation of parameters pertaining to the cleaning unit, yet they fail to adequately address the issue of material accumulation at the rear of the sieve surface.

In conclusion, this paper employs a coupled simulation approach combining CFD and DEM with practical experiments to simulate and validate the cleaning unit of a crawler-type combine harvester. The objective of this study is to enhance the efficiency of the cleaning process, reduce the impurity rate, and minimise the loss rate. This will be achieved through the design of the pre-screening device and the optimisation of the cleaning system parameters. Ultimately, this will determine the optimal working parameters for the cleaning unit of the crawler-type combine harvester and identify the optimal structure for the pre-screening device.

MATERIALS AND METHODS
Principle design of simulation structure

The cleaning device represents a fundamental component of the combine harvester, comprising a fan, vibrating screen, grain auger, residual auger, and pre-screening device. Upon initiation of operation, the cleaning screen and oscillating plates engage in a reciprocating motion, enabling the sequential conveyance of material from the upper oscillating plate through the middle one to the lower oscillating plate. During this process, the fan generates an airflow that expels the majority of lightweight impurities from the machine. The combination of the fish-scale and woven screens on the vibrating screen facilitates a more efficient and dispersed separation process. During the cleaning process, the wheat grains are conveyed to the grain bin by the grain auger, while any non-grain impurities are directed to the secondary cleaning stage via the residual auger. This mechanism serves to guarantee the quality of the grains, while also markedly enhancing the efficiency of the harvesting process, as illustrated in Figure 1.
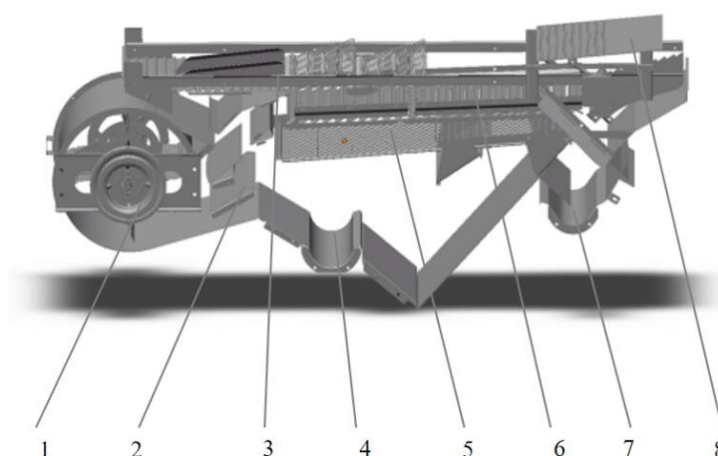

Fig.1 Structure of the cleaning device
1. Blower; 2. Dividing plate; 3. Upper shaking plate; 4. Seed conveying device; 5. Lower sieve woven sieve;
6. Fish scale sieve; 7. Debris conveying device; 8. Pre-screening device

The pre-screening device comprises a crank mechanism, comprising a drive motor, slide rails, a support

frame and a crank arm. The implementation of a pre-screening process at the rear of the cleaning system has the potential to significantly reduce material accumulation on the screen surface, thereby decreasing the overall working load of the vibrating screen and subsequently enhancing the efficiency of the cleaning process. The installation of the pre-screening device at the rear end of the concave sieve of the combine harvester allows for the effective pre-cleaning of the rear-end mixture of wheat. The pre-cleaning operation has the effect of significantly alleviating the workload of the vibrating screen. Consequently, the majority of the wheat mixture can be transferred to the central area of the vibrating screen, where cleaning efficiency is higher. Furthermore, the pre-screening device guarantees the uniform distribution of impurities across the screen surface, thus preventing the accumulation of materials caused by impurities directly falling onto the screen. This not only optimises the handling of impurities but also effectively prevents grains that have not been adequately processed from being discharged at the rear of the machine, thereby reducing losses during the cleaning process, as illustrated in Figure 2.
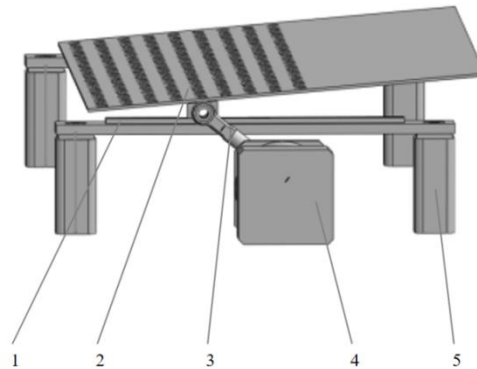

Fig. 2 - Pre-screening device
1. Pre-screen plate slide; 2. Pre-screen plate; 3. Curved arm; 4. Drive motor; 5. Support structure

Establishment of the Simulation Model Structure

In order to reduce the amount of computational energy consumed and to enhance the speed of the simulation, the model was simplified during its construction. The three-dimensional modelling software SolidWorks was employed to create a simplified representation of the cleaning section, retaining only those components that significantly impact the cleaning process, such as the oscillating plate, upper screen, and lower screen. With regard to dimensions, apart from a reduction in the width of the cleaning chamber, all other measurements were based on the actual dimensions of the harvester in real-world settings, with the exception of the aforementioned simplification.

In particular, the length of the cleaning chamber is 2000 mm, with a width of 720 mm and a height of 800 mm. The oscillating plate has a length of 540 mm and is situated 200 mm from the top of the cleaning chamber. The upper vibrating screen is composed of 20 fish-scale screens, whereas the lower screen employs a woven mesh design, measuring 860 mm in length and 735 mm in width. The apertures in the screen are square in shape, measuring 1.8 mm by 1.8 mm, with a distance of 2 mm between units. The distance between the upper screen and the lowest point of the oscillating plate is 160 mm, while the gap between the upper and lower screens is 200 mm. The upper and lower screens are of identical thickness, measuring 1 mm.

Simulation of the mathematical model and the parameters settings
Establishment of the Wheat Threshing Material Discrete Element Model

A discrete element model (DEM) for wheat threshing material was developed with the objective of simulating the behaviour of particles during the cleaning process. The objective of the model was to accurately represent the physical properties of wheat grains, chaff, and other impurities, which are crucial for understanding the separation mechanism in the cleaning system.

The construction of the DEM model for wheat threshing material necessitated the determination of the physical properties of the material's various components. The triaxial dimensions of wheat grains, when placed horizontally, were found to be 6.20-6.76 mm in length, 2.50-2.98 mm in width, and 2.30-2.98 mm in thickness, as indicated by the measurements. The mean values for length, width, and thickness were found to be 6.76 mm, 2.98 mm, and 2.88 mm, respectively.

The length of the short stalks ranged from 12.65 mm to 83.22 mm, with an outer diameter of 1.27 mm

to 3.23 mm and a wall thickness of 0.32 mm to 0.55 mm. The mean values for short stalk length, outer diameter, and wall thickness were found to be 22.95 mm, 2.21 mm, and 0.41 mm, respectively.

The discrete element modelling method was employed to model the various components of the threshed wheat material, which mainly consisted of grains and short stalks, using the triaxial dimensions of wheat grains as a basis. To guarantee the veracity and precision of the simulation experiments, models were constructed for all components, and the multi-sphere particle filling method in EDEM software was employed to streamline, overlap, and populate the particle models of each component. This approach yielded discrete element models of the various components of the wheat threshing material, as illustrated in Figure 3.
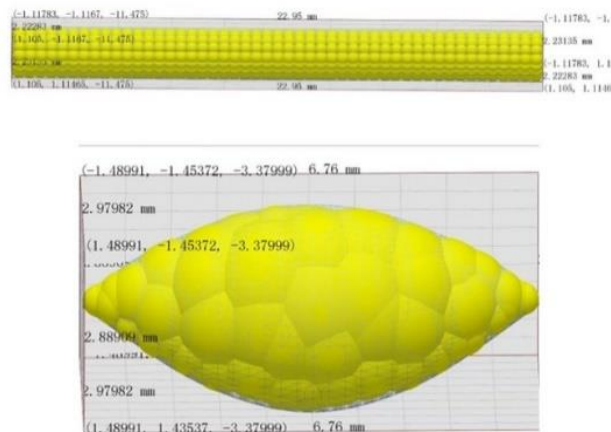

Fig. 3 - Discrete meta-model of wheat exudates

Physical Properties and Contact Parameters of Wheat Threshing Material

In accordance with the findings of prior research and the outcomes of pertinent experiments, the attribute parameters of the discrete element model for the diverse components of the wheat threshing material throughout the simulation process are presented in Table 1. The interaction parameters of each material are shown in Table 2.

Table 1

Material properties

Material	Poisson's ratio	Shear modulus（MPa）	Density（kg/m³）
grain	0.3	2.6	1350
Short stems	0.4	1	104
Cleaning room	0.3	7800	7800

Table2

The interaction parameters of each material

Contact form	Material coefficient	Coefficient of static friction	Rolling friction coefficient
Grains - Grains	0.2	1.00	0.01
Grains - short stems	0.3	0.5	0.01
Grain-cleaning chamber	0.45	0.35	0.01
Short stalk - short stalk	0.22	0.5	0.01
Short stalk - cleaning	0.3	0.36	0.01

The wheat grain mass constitutes 90.32% of the total mass of the threshed material, while short stalks account for 4.18%, and light impurities account for 5.5%. The impurities present in wheat grains are primarily composed of short stalks, while light impurities (such as dust, wheat husks, and fragmented leaves) are frequently dislodged from the grain and rarely accumulate in the grain tank beneath the cleaning apparatus.

Accordingly, subsequent research will not consider these light impurities as subjects for investigation,

and will instead focus on the impact of short stalks. This is due to the fact that the primary impurities present in the grain tank during the cleaning process are short stalks.

Simulation of the mathematical model
Particle collision model

In order to accurately simulate the collisions between particles, as well as between particles and the screen surface, the Hertz-Mindlin (no-slip) contact model was employed within the EDEM software. The motion of the particles was determined in accordance with the mechanical equilibrium equations.

$$\mathrm{m_p} \frac{d\mathrm{v_p}}{d\mathrm{t}} = F_D + F_{GB} + F_{SA} + F_{Ma} \tag{1}$$

$$I_p \frac{d\omega_t}{d_t} = T \tag{2}$$

In the formula:

m_p represents the particle mass (kg); V_p represents the particle velocity; t—the total simulation time (s); F_D—the drag force (N); F_{GB}—the gravitational force (N); F_{Sa}—the Saffman lift force (N); F_{Ma}—the Magnus lift force (N); I_p— the moment of inertia of the particle; w_n— the angular velocity of the particle (rad/s); T—the torque acting on the particle (N·m)

Fluid-phase control mode
Simulation of parameter settings

In the single-factor simulation experiments, the simplified device model was imported into the EDEM software, and the material properties of the sieve box and sieve plate were specified. Additionally, the motion parameters of the sieve box were set. In the course of the simulation, the Hertz-Mindlin no-slip contact model was utilised. A particle factory was positioned above the oscillating plate and configured to generate wheat grain and short stalk models as previously defined. The particle factories were configured to generate these components in a dynamic manner, with a total of 2,000 wheat grains and 400 short stalks. In the single-factor airflow velocity experiment, the CFD-DEM coupling method was employed to investigate the impact of airflow velocity on the experimental outcomes.

In this simulation, EDEM was coupled with Fluent, with the Hertz-Mindlin (no-slip) contact model selected in EDEM. The simplified cleaning device model was imported into EDEM, where the particle models were created. A particle factory was positioned directly above the oscillating plate. In Fluent, the ANSYS Workbench Design Modeler was employed to streamline the model and obtain the internal flow channel computational domain. Furthermore, in the Meshing module, an unstructured tetrahedral mesh was utilised to discretise the cleaning system model. Once all the requisite parameters had been set, the simulation experiments were initiated.

RESULTS

The findings of existing research indicate that the fan speed of the airflow-sieve cleaning device, in conjunction with the structural and dynamic parameters of the vibrating screen, exert a considerable influence on the efficacy of the device in terms of cleaning performance. Accordingly, this study has selected three experimental factors for analysis in the context of the cleaning device of the tracked rice-wheat combine harvester: fan speed, vibrating screen frequency, and vibrating screen amplitude. The evaluation indices for the single-factor experiments were the grain impurity content and cleaning loss rate. These indices were subjected to analysis with the objective of evaluating the operational performance of the cleaning device under different working parameters, with a view to determining the optimal combination of working parameters.

A review of the relevant literature and prior experimental data informed the decision-making process regarding the scope of the single-factor experiments. The fan speed was set between 8 m/s and 12 m/s, the reciprocating vibrating screen frequency ranged from 6 to 10 Hz, and the vibration amplitude was set between 20 mm and 40 mm. In the course of the simulation trials, two factors were maintained at a constant level in each experiment in order to investigate the impact of these parameters on the operational performance of the airflow-sieve cleaning device of the tracked combine harvester.

The influence of fan speed on the cleaning result

A simulation analysis was conducted to investigate the impact of fan speed on cleaning efficiency under

conditions where the vibrating screen frequency was set at 9 Hz and the screen amplitude at 35 mm. The fan speed was adjusted to 8 m/s, 9 m/s, 10 m/s, 11 m/s, and 12 m/s to observe the behaviour of the wheat threshing mixture within the cleaning device, with the objective of determining the optimal fan speed range. Following the simulation, the data pertaining to the impurity content and cleaning loss rate were duly recorded.

As the fan speed increased during the simulation, the force exerted on the threshed material in the airflow field also increased. This resulted in a prolonged suspension time and a backward shift in the position where the material landed on the screen. This resulted in an increase in wheat grain losses. At relatively low fan speeds, the threshed material fell rapidly onto the screen surface, resulting in a reduction in the quantity of blown-off impurities and an increase in the impurity content of the grains. However, the grains remained at a greater distance from the discharge port, thus reducing the probability of their loss and maintaining a low cleaning loss rate.

As illustrated in the accompanying figure 4, the gradual increase in fan speed was accompanied by a decrease in the impurity content of the wheat, while the cleaning loss rate exhibited a gradual increase. In the fan speed range of 8 m/s to 9 m/s, the impurity content decreased from 4.31% to 3.01%, indicating effective removal of light impurities within this range. Meanwhile, the cleaning loss rate remained at a relatively low level of approximately 1.7%. Upon further increasing the fan speed to 10 m/s, the impurity content decreased to 1.89%, while the cleaning loss rate rose to 2.51%. This resulted in an intersection point between the two trends.

Further increases in fan speed to 11 m/s and 12 m/s resulted in a reduction in impurity content to 1.16% and 0.95%, respectively. However, this was accompanied by an increase in cleaning loss rate, which reached 3.99% and 5.21%, respectively. This trend suggests that, within a certain range, an increase in fan speed effectively separates impurities, resulting in a gradual reduction in impurity content. However, when the fan speed exceeded 10 m/s, the excessive airflow intensity resulted in a greater likelihood of the wheat grains being blown off the screen, leading to a notable increase in the loss rate. In light of the observed variations in impurity content and cleaning loss rate, it can be inferred that the optimal fan speed range is likely to be between 9 m/s and 10 m/s, where the impurity content is relatively low and the loss rate is kept at a minimum level.
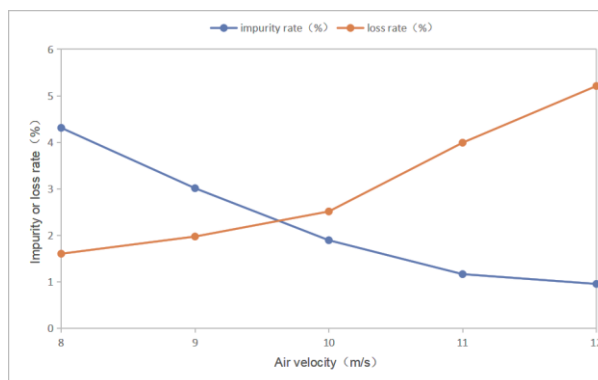

Fig. 4 - Schematic diagram of cleaning results

The influence of the vibrating frequency of the shaker on the sorting result

A simulation analysis was conducted to investigate the effect of vibrating screen frequency on cleaning performance for wheat. The vibrating screen amplitude was set at 30 mm and the fan speed at 10 m/s, with frequencies ranging from 6 to 10 Hz. The simulation results indicated that as the vibration frequency increased, the velocity of the threshed material also increased, while the residence time of the material on the screen surface decreased accordingly. This consequently reduced the probability of the material passing through the screen mesh. Upon contact with the screen, the high vibration frequency caused the material to scatter with ease and gain significant initial velocity, rendering it more susceptible to ejection from the cleaning chamber by the fish-scale screen. Consequently, the grain loss rate increased, while the proportion of grains in the screened material decreased, resulting in an elevated impurity content.

Further analysis demonstrated that, as illustrated in the figure 5, an increase in the vibrating screen frequency resulted in a gradual upward trend in the cleaning loss rate, while the grain impurity content initially exhibited a decrease and then an increase. As the vibration frequency increased from 6 Hz to 10 Hz, the cleaning loss rate exhibited a notable rise from 2.41% to 3.02%. Concurrently, the impurity content demonstrated a decline from 3.21% to 2.15%.

However, this trend reversed, with the cleaning loss rate rising once more to reach 2.34%. This can be attributed to the increased jumping frequency of wheat grains under higher vibration frequency, as well as their

accelerated horizontal velocity, which increased the likelihood of them jumping directly towards the discharge port, resulting in increased losses. Furthermore, as the loss rate increased, the proportion of wheat grains in the screened material decreased, resulting in an elevated impurity content. In conclusion, the optimal cleaning effect was achieved when the vibration frequency was between 8 Hz and 9 Hz, as this resulted in the lowest impurity content and cleaning loss rate.
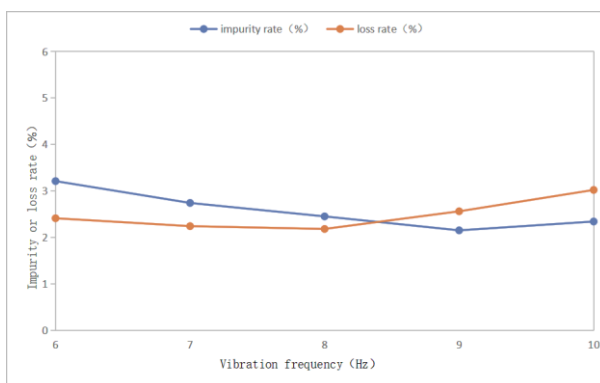

Fig. 5 - Schematic diagram of cleaning results

The Influence of Vibrator Amplitude on Sorting Results

The objective of this investigation was to ascertain the impact of vibrating screen amplitude on cleaning performance for wheat. To this end, different amplitude settings were applied to a simulation model under conditions of a fan speed of 10 m/s and a vibration frequency of 9 Hz. The amplitudes simulated included 20 mm, 25 mm, 30 mm, 35 mm, and 40 mm, with the objective of observing the behaviour of threshed wheat material on each screen surface and determining the optimal amplitude range. As illustrated in Figure 6, the numerical simulation results demonstrated that an amplitude of 30 mm resulted in an even distribution of the threshed wheat material on the screen, thereby achieving optimal sieving performance. Furthermore, this amplitude setting minimised both the grain loss rate and impurity content.

Conversely, at an amplitude of 30 mm, the sieving effect of the threshed wheat material on both the upper and lower screen surfaces was optimal, with minimal grain loss and the highest cleaning efficiency, resulting in stable operational performance. In conclusion, the results demonstrated that an amplitude of 30 mm was able to maintain a low loss rate while effectively reducing impurity content, achieving the best cleaning performance under the given fan speed and vibration frequency conditions.
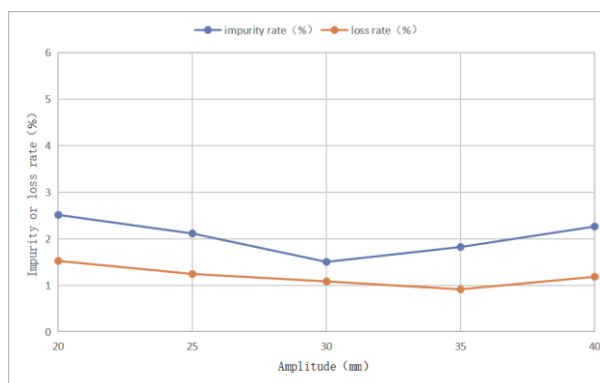

Fig. 6 - Schematic diagram of cleaning results

Pre-screening device structure optimisation

The CFD simulation analysis yielded two main conclusions regarding the airflow field distribution within the cleaning chamber. Firstly, the airflow velocity was observed to be relatively low in the area above the twentieth fish-scale screen. Secondly, a similarly low airflow velocity was observed in the area above the tenth fish-scale screen from the end as illustrated in Figure 7. In light of these findings, the structure and dimensions of the pre-screening plate were subsequently optimised.

In order to prevent the accumulation of wheat threshed material in a single area of the screen, which could result in an increased load, the pre-screening device's screen plate was designed to consist of a return plate and a perforated screen.

The wheat threshed material that falls from the end of the concave screen is propelled forward by the return plate. A proportion of the threshed material is able to pass through the perforated screen and fall onto

the surface of the vibrating screen in advance, thereby performing a pre-cleaning function. The material that does not pass through continues to move forward and ultimately falls onto the vibrating screen surface from the end of the perforated screen.

The dimensions of the screen plate were determined based on the width of the cleaning chamber, which was set at 810 mm, while the length was established as 4000 mm, according to the distance from the twentieth fish-scale screen to the machine outlet. The width of the perforated screen within the screen plate is identical to that of the screen plate itself, with a total length of 215 mm. This distance is determined by the distance from the tenth fish-scale screen from the end to the vibrating screen outlet, with the return plate measures 185 mm in length. The diameter of the perforations in the screen was determined based on the average length of the short stalks present in the threshed material, with a final measurement of 12 mm established.
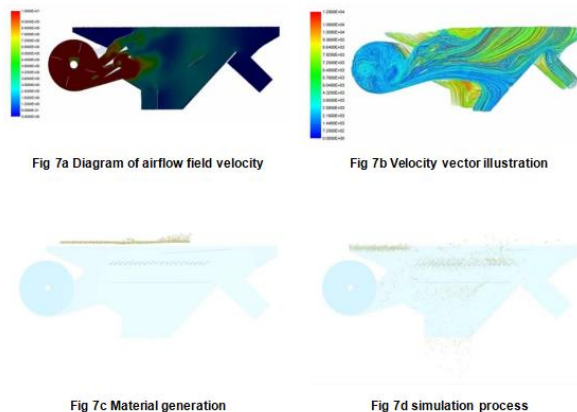

Fig 7a Diagram of airflow field velocity   Fig 7b Velocity vector illustration

Fig 7c Material generation   Fig 7d simulation process

Fig. 7 - Selection simulation process

Orthogonal test numerical simulation and result analysis
Orthogonal experimental results

An orthogonal coupled simulation experiment was conducted, in which fan speed, vibration frequency and amplitude were identified as factors, with impurity content and grain loss rate of wheat kernels identified as evaluation indices. In accordance with the findings of the single-factor experiment detailed, the optimal intervals for these three parameters were identified and selected for further orthogonal simulation, as shown in Table 3.

Table 3

Virtual Orthogonal Experiment Factors and Level Table

Level	Test Factors		
	A airflow velocity (m/s)	B oscillation (Hz)	C amplitude (mm)
1	9	7	25
2	10	8	30
3	11	9	35

Analysis of the contamination rate results

Table 4

Experimental plan and results

Number	A airflow velocity （m/s）	B oscillation （Hz）	C amplitude （mm）	Trash content （%）	Loss rate （%）
1	9	7	25	3.51	2.60
2	9	8	30	3.12	2.00
3	9	9	35	2.61	1.94
4	10	7	30	3.19	2.51
5	10	8	35	2.80	2.12
6	10	9	25	3.72	2.20
7	11	7	35	2.30	1.73
8	11	8	25	3.03	1.91
9	11	9	30	2.10	1.62

Table 5

Analysis of Impurity Rate Range

Serial number	A airflow velocity （m/s）	B oscillation （Hz）	C amplitude （mm）

K1	12.0	10.5	10.7
K2	9.5	9.2	8.1
K3	7.8	8.6	9.5
K1	4.0	3.5	3.57
K2	3.17	3.07	2.7
K3	2.6	2.87	3.17
range	1.4	0.63	0.87
Primary and secondary factors	airflow velocity (A) > oscillation **(B)** > amplitude **(C)**		
Optimization plan	airflow velocity **(A)**:=9m/s oscillation **(B)**= 25mm amplitude **(C)**= 7Hz		

As demonstrated in table 4 and table 5, a reduction in impurity content is associated with enhanced cleaning efficiency. A range analysis of the various factors revealed that airflow velocity (A) had the most significant impact on impurity content, with the lowest impurity content observed at an airflow velocity of 9 m/s. The second most influential factor was amplitude (B), with an amplitude of 25 mm demonstrating the optimal cleaning effect. Vibration frequency (C) was found to exert the least influence on impurity content, with a frequency of 7 Hz yielding favourable results. It can therefore be concluded that the order of influence on impurity content is as follows: airflow velocity > amplitude > vibration frequency. In light of the aforementioned findings, the optimal parameter combination for minimising impurity content and maximising cleaning efficiency in the cleaning process is an airflow velocity of 9 m/s, an amplitude of 25 mm, and a vibration frequency of 7 Hz.

Table 6

Analysis of Variance with Impurity Rate

	Type III sum of squares	df	mean square	F	Sig
Correction model	8.960	6	1.493	296.670	0.003
Intercept	46.444	1	46.444	9124.312	0.000
Airflow velocity	8.361	2	4.180	418.119	0.001
Vibration frequency	0.541	2	0.270	27.356	0.024
Amplitude	0.299	2	0.150	15.534	0.046
Error	0.021	2	0.010		
Total	56.414	9			
Total of corrections	8.970	8			

Table 6 presents the analysis of variance (ANOVA) for impurity content following the completion of the orthogonal experiments. In accordance with the F distribution table, the critical value is $F_{0.05}(2,2) = 19$. As illustrated in the table, the F-values for airflow velocity, vibration frequency, and amplitude are all greater than $F_{0.05}(2,2) = 1$. This suggests that there is a significant impact of airflow velocity, vibration frequency, and amplitude on impurity content. The F values indicate that airflow velocity has the greatest influence on impurity content, followed by vibration frequency and then amplitude. This finding is in accordance with the conclusions previously drawn from the range analysis.

Analysis of loss rate results

Table 7

Loss Rate Range Analysis

Serial number	A airflow velocity（m/s）	B oscillation（Hz）	C amplitude（mm）
K1	7.6	7.3	6.8
K2	6.9	6.3	6.5
K3	5.5	6.4	6.7
K1	2.53	2.43	2.27
K2	2.3	2.1	2.17
K3	1.83	2.13	2.23
range	0.7	0.33	0.1
Primary and secondary factors	airflow velocity (A) > oscillation (B) > amplitude (C)		
Optimization plan	airflow velocity (A):=11m/s oscillation (B)= 30mm amplitude (C)= 9Hz		

A review of the data in the table reveals a clear correlation between the loss rate and the cleaning effect: the lower the loss rate, the more effective the cleaning. The range analysis of the various factors indicates that airflow velocity (A) exerts the most significant influence on the loss rate, with the lowest loss rate occurring at an airflow velocity of 11 m/s.

The subsequent most influential factor is amplitude (B), whereby a 30 mm amplitude is observed to yield the optimal cleaning effect. Vibration frequency (C) exerts the least influence on the loss rate, with the optimal

performance observed at 9 Hz. Therefore, the order of influence on loss rate among airflow velocity, amplitude, and vibration frequency is as follows: airflow velocity > amplitude > vibration frequency. It can therefore be concluded that the optimal parameter combination for minimising the loss rate during the cleaning process is an airflow velocity of 11 m/s, an amplitude of 30 mm, and a vibration frequency of 9 Hz, which yields the lowest loss rate and the best cleaning effect.

Table 8

Loss rate variance analysis table

	Type III sum of squares	df	mean square	F	Sig
Correction model	0.926	6	0.154	297.513	0.003
Intercept	48.780	1	48.780	11745.231	0.000
Airflow velocity	0.683	2	0.342	243.154	0.001
Vibration frequency	0.273	2	0.136	136.385	0.005
Amplitude	0.089	2	0.045	91.000	0.011
Error	0.021	2	0.010		
Total	50.866	9			
Total of corrections	0.926	8			

The conclusions shown in Table 8 are consistent with the conclusions drawn in Table 6.

Comprehensive analysis of loss rate and impurity rate

In the cleaning system, the effects of airflow velocity, feed rate, and vibration frequency on impurity content and cleaning rate are significant, resulting in an inverse relationship between impurity content and cleaning rate. Accordingly, in order to achieve equilibrium between these two pivotal indicators and to enhance the efficacy of the cleaning process, the comprehensive weighted average methodology is employed to evaluate the simulation outcomes pertaining to impurity content and cleaning rate. The calculation method is as follows:

$$Z_i = W_1 \times \frac{y_{i1}}{y_{1max}} + W_2 \times \frac{y_{i2}}{y_{2max}} \qquad (3)$$

In the formula:

Z_i—Weighted score for the *i*-th experiment; W_1—Weight of impurity content, W_1=30%;

W_2—Weight of loss rate, W_1=70%, y_{i1}—Impurity rate of the *i*-th experiment;

y_{1max}—Maximum impurity content in the experiment; y_{i2}—Loss rate of the *i*-th experiment;

y_{2max}—The maximum loss rate in all experiments

Table 9

Weighted score of two evaluation indicators

Number	A airflow velocity （m/s）	B oscillation （Hz）	C amplitude （mm）	Trash content （%）	Loss rate （%）	Weighted score
1	9	7	25	3.51	2.60	98.306
2	9	8	30	3.12	2.00	79.007
3	9	9	35	2.61	1.94	73.279
4	10	7	30	3.19	2.51	93.303
5	10	8	35	2.80	2.12	79.658
6	10	9	25	3.72	2.20	91.923
7	11	7	35	2.30	1.73	65.125
8	11	8	25	3.03	1.91	80.973
9	11	9	30	2.10	1.62	60.550

A lower weighted score is indicative of a lower impurity content and loss rate, thereby indicating an enhanced cleaning performance. As illustrated in the aforementioned table, Experiment 9 has the lowest weighted score of 60.550, thereby identifying it as the optimal parameter combination. The optimal parameter combination is as follows: airflow velocity A = 11 m/s, vibration frequency B = 9 Hz, and amplitude C = 30 mm.

CONCLUSION

The objective of this study was to develop a novel pre-screening device to address the limitations of traditional cleaning systems during grain harvesting, specifically the issues of cleaning efficiency and grain loss. The device effectively alleviates the accumulation of material on the sieve surface, thereby significantly enhancing the separation of material.

The pre-screening device has the effect of reducing the workload of the cleaning mechanism, thereby improving the efficiency of the cleaning process and the overall performance of the harvesting operation. This

design optimisation not only enhances the operational stability of the cleaning mechanism but also provides a novel reference point for the future development of combine harvesters.

The optimal parameter combination for the cleaning mechanism is as follows: A CFD-DEM simulation analysis was conducted to determine the optimal operating parameters for the cleaning system. A comprehensive analysis of airflow velocity, vibration frequency, and amplitude led to the conclusion that the optimal combination for cleaning performance is an airflow velocity of 11 m/s, a vibration frequency of 9 Hz, and an amplitude of 30 mm. This combination ensures an optimal balance between a low impurity rate and a low grain loss, thereby significantly enhancing the overall cleaning performance of the combine harvester during field operations.

REFERENCES

[1]   Badretdinov, I., Mudarisov, S., Lukmanov, R., Ibragimov, R., Permyakov, V., Tuktarov, M, (2020). Mathematical modeling and study of the grain cleaning machine sieve frame operation, *INMATEH – Agricultural Engineering,* vol.60(1), 19-28.

[2]   Chen, S., (2021). Simulation and key parameters optimisation of wheat harvester clearing based on CFD-DEM (基于 CFD-DEM 小麦收获机清选仿真与关键参数优化). *Jinan University*.

[3]   Christian, K., Thomas, H., (2017). Coupled CFD-DEM Simulation of Separation Process in Combine Harvester Cleaning Devices. *Landtechnik*, Vol. 72, No. 5.

[4]   Dai, F., Song, X. F., Zhao, W. Y., (2019). Motion simulation and test on threshed grains in tapered threshing and transmission device for plot wheat breeding based on CFD-DEM. (基于 CFD-DEM 的小麦育种锥形脱粒和传输装置中的运动模拟和脱粒测试). *International Journal of Agricultural and Biological Engineering*, 12(1): 66-73.

[5]   Li D.J., Hou, J.L., Wang, D.W., Chang, Z.J., (2024). Design and testing of peanut sieving prototype machine. *INMATEH –Agricultural Engineering,* 73(2), 760-770.

[6]   Guo, S.J., Ma, X.D., Liu, Z.H., Chen, G.H., Wang, S., (2021). Simulation study and parameter discussion of wind sieve type grain cleaning. (风筛式谷物清选模拟研究及参数讨论). *Agricultural Mechanisation Research*, 43(02): 10-15.

[7]   Han, D.D., Zhang, D.X., (2018). DEM-CFD coupling simulation and optimization of an inside-filling air-blowing maize precision seed-metering device. (DEM-CFD 耦合模拟与优化玉米精准播种装置). *Computers and Electronics in Agriculture*, 150: 426-438.

[8]   Han, D.D., Zhang, D.X., Jing, H.R., Cui, T., Yang, L., (2018). DEM-CFD coupling simulation and optimization of an inside-filling air-blowing maize precision seed-metering device (DEM-CFD 耦合模拟和优化内部填充式吹气玉米精密种子计量装置). *Computers and Electronics in Agriculture*, 150: 426-438.

[9]   Ii, Y.M., Zhao, Z., Chen, J., Xu, L. Z. (2007). Nonlinear motion law of material on air-and-screen cleaning mechanism (风筛式清选装置上物料的非线性运动规律). *Transactions of the Chinese Society of Agricultural Engineering*, 23(11): 142-147.

[10]   Li, H.Z., Li, Y.M., Tang, Z., (2011). Numerical simulation and analysis of shaker simulation based on EDEM (基于 EDEM 的振动筛仿真数值模拟与分析). *Transactions of the Chinese Society of Agricultural Engineering*, 27(5): 117-121.

[11]   Li, H.C., Li, Y.M., Tang, Z., Xu, L.Z., (2012). CFD-DEM numerical simulation of material movement on the vibrating screen of the air sieve cleaning device (风筛式清选装置振动筛上物料运动 CFD-DEM 数值模拟). *Transactions of the Chinese Society of Agricultural Engineering*, 43(2): 79-84.

[12]   Liang, Z.W., LI, Y.M., Ma, P.P., Wei, C.C., Wang, J.P., (2018). Structural optimisation and test of the cleaning device of longitudinal flow combine harvester.（纵轴流联合收获机清选装置结构优化与试验）. *Research on Agricultural Mechanisation*. 40(05): 170-174.

[13]   Mircea, C., Nenciu, F., Vlăduţ, V., Voicu, Gh., Gageanu, I., Cujbescu, D. (2020), Increasing the performance of cylindrical separators for cereal cleaning, by using an inner helical coil. *INMATEH – Agricultural Engineering,* vol.62(3), 249-258.

[14]   Ning, X.B.，Xu, I., Sun, C.H., Yang, H.S., (2019). Fan's parameters optimization and internal flow field distribution in multi-duct cleaning device of combine harvester *(*联合收获机多风道清选装置气流场分布与风机参数优化) *Journal of Agricultural Mechanization Research*, 41(6):32-37.

[15]   Tang, X.H., Zhao, N., Guo, B., Jin, C.Q., Yu, M. Q., Li, J.Q., Qing, B., (2022). Design and test of multi-parameter adjustable cleaning loss distribution inspection test bench (多参数可调式清选损失分布检则

试验台设计与试验). *Research of Agricultural Mechanisation*, 44(12): 148-155.

[16]   Wang, J., Li, Z., Hussain, S., Lu, Q., Song, H., Zheng, D, (2020). Design and threshing outputs study of internal and external rotary roller buckwheat thresher, *INMATEH –Agricultural Engineering,* vol.60(1), 173-182.

[17]   Liu, L. W., Liu, F., Wei, C. Y., Peng, F., Wang, J.Q., (2024). Design and simulation analysis of the tuber harvest screening machine. *INMATEH –Agricultural Engineering,* vol.73(2), 534-545.

[18]   Xiao, X.X., Li, B., Wu, C.Y., Qi, X.D., Hu, T., (2018). Motion analysis of the cylindrical sieve cleaning process of two early rice varieties based on DEM-CFD. (基于 DEM-CFD 两种早稻品种圆筒筛清选过程的运动分析). *Mechanical Design*, 35(10): 32-37.

[19]   Xu, L.Z., Yu, L.J., LI, Y.M., Ma, Z., Wang, C.H., (2014). Numerical simulation of the internal flow field of a double outlet multiduct centrifugal fa. (双出风口多风道离心风机内部流场数值模拟). *Journal of Agricultural Machinery*, 45(10): 78-86.

[20]   Yuan, Z.X., DAI, F., ZHAO, W.Y., Shi, R.J., Zhao, Y.M., (2023). Simulation analysis and test of CFD-DEM based air-screen cleaning device for huisache (基于 CFD-DEM 的胡麻风筛式清选装置仿真分析与试验). *Agricultural Research in Arid Regions,* 41(06):281-290.

[21]   Zhao, Z., Yang, X., Zhang, G., (2022). Analysis and optimization test of operation process of cleaning device of corn seed harvester, *INMATEH –Agricultural Engineering,* vol.68(3), 211-220;

[22]   Zhu, P. F., (2019). Simulation research on grain air-and-screen cleaning process and optimization of key parameters. (谷物风筛清选仿真研究及关键参数优化设计). *Hangzhou: Zhejiang University*.

[23]   Zhang, H., Wang, Z., & Zhao, J, (2022). Simulation of grain cleaning process in combine harvester using CFD-DEM coupling method. *Biosystems Engineering*, 204, 53-65.